Int J Adv Manuf Technol (2014) 71:1901–1908
DOI 10.1007/s00170-014-5633-x

ORIGINAL ARTICLE

Analytical modeling of adiabatic shear band spacing for serrated chip in high-speed machining

Qibiao Yang · Zhanqiang Liu · Zhenyu Shi · Bing Wang

Received: 5 September 2013 / Accepted: 13 January 2014 / Published online: 28 January 2014

Abstract Theoretical prediction of adiabatic shear band spacing is beneficial to understand the mechanism of the serrated chip formation. The momentum equation, energy equation and compatibility equation in orthogonal cutting are established in this paper. Using perturbation analysis by regarding cutting speed and uncut chip thickness as basic disturbance, an analytical solution of adiabatic shear band spacing is developed. Adiabatic shear band spacing of serrated chip is related to the wave number of the perturbation when the growth rate reaches to maximum. It is found that adiabatic shear band spacing decreases with the increase of cutting speed but increases with uncut chip thickness. The experiment of orthogonal cutting Ti6Al4V under different cutting speeds (50 m/min-1800 m/min) and uncut chip thicknesses (0.02 mm-0.16 mm) verifies the validity of the theoretical prediction.

Keywords Orthogonal cutting · Adiabatic shear band spacing · Serrated chip · Perturbation analysis

Q. Yang
School of Mechanical Engineering, Hubei University of Technology, Wuhan 430068, People's Republic of China

Z. Liu (✉) · Z. Shi · B. Wang
School of Mechanical Engineering, Shandong University, Jinan 250061, People's Republic of China
e-mail: melius@sdu.edu.cn

Z. Liu · Z. Shi · B. Wang
Key Laboratory of High Efficiency and Clean Mechanical Manufacture, Ministry of Education, Shandong University, Shandong, People's Republic of China

1 Introduction

The serrated chip is prone to forming in high-speed machining. While the workpiece material is plastic metal, the mechanism of serrated chip could be expressed as an adiabatic shear instability. The characteristic of adiabatic shear is that there are some narrow bands due to severe plastic deformation. These narrow bands are usually called adiabatic shear band (ASB). Figure 1 presents ASB in serrated chip during high-speed machining Ti6Al4V under the cutting conditions of cutting speed V= 1,200 m/min, uncut chip thickness a_c=0.07 mm, tool rake angle γ_0=0°, and cutting speed V=4800 m/min, uncut chip thickness a_c=0.035 mm, tool rake angle γ_0=0° [1]. Adiabatic shear band spacing (ASBS) is an important geometric characteristic of serrated chip. Prediction of ASBS is conducive to understand the mechanism of serrated chip formation such as accurately calculating the frequency of serrated chip.

The analytical method to predict ASBS is mostly used by impact tests. Batra and Kim analyzed the nonlinear coupled partial differential equations governing the overall simple shearing deformations of a thermal-softening viscoplastic block. The effect of the defect size on the initiation and subsequent growth of the shear band has been studied [2]. Wright and Ockendon have used linear perturbation analysis to characterize adiabatic shear instability. It is assumed that the wavelength associated with the dominant mode determines ASBS. The analysis of this is restricted to perfect plastic materials without considering strain hardening [3]. Batra and Chen studied the thermo-viscoplastic response of the material by four different relations using perturbation method. The stability of the governing equations is analyzed [4]. It is found that the qualitative responses predicted by Wright–Batra, Johnson–Cook and power law relations are similar but they differ from that predicted by Bodner–Partom relation. Molinari has characterized ASBS by analytical methods with one-dimensional formulation. Using perturbation analysis, a

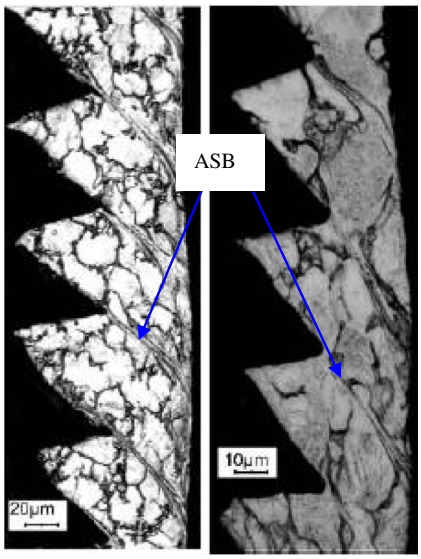

V=1200m/min	V=4800m/min
a_c=0.07mm	a_c=0.035mm
γ_0=0°	γ_0=0°

Fig. 1 ASBS in high-speed orthogonal machining Ti6Al4V [1]

dominant instability mode whose wavelength is related to ASBS has been characterized. Explicit solutions for materials with no strain hardening have been found. Asymptotic developments have been used to obtain the results considering strain hardening [5]. Based on Molinari's model [5], Yang et al. proposed a modified model of ASBS by considering the non-uniform distribution of the wavy plastic deformation. A shape factor is introduced to represent the effect of applied loads and the pre-deformation on shear band spacing [6]. Batra and Wei developed an analytical model of ASBS for the thermo-viscoplastic materials considering strain hardening, strain-rate hardening, and thermal softening by studying the stability of a homogeneous solution of equations governing its simple shearing deformations. They found that ASBS increases with thermal conductivity and strain-rate hardening exponent but it decreases with an increase of strain-hardening exponent [7]. Through high-speed machining of 1045 steel, the influence of cutting speed on the chip formation was studied. The quantitative relationship between chip morphology parameters and the cutting speed has been obtained [8].

ASB is usually generated in high frequency during high-speed cutting processes. As shown in Fig. 1, the thickness of the shear zone is small and kinetic. The variation of ASBS can be ascribed to the change of cutting conditions such as cutting speed and uncut chip thickness. In this paper, a closed-form expression of ASBS in high-speed machining is proposed using perturbation analysis. The effects of cutting conditions including cutting speed and uncut chip thickness on ASBS are studied. Through high-speed machining Ti6Al4V, the method to obtain the analytical solution of ASBS is confirmed.

2 Modeling of high-speed orthogonal cutting

For developing the model of high-speed orthogonal cutting, the following assumptions are made:

1. The orthogonal cutting process is under plane strain deformation conditions.
2. There is no build-up edge (BUE) formation in orthogonal cutting.
3. The radius of cutting edge is neglected.
4. The workpiece material is supposed to be homogeneous that is isotropic hardened and governed by thermo-viscoplastic constitutive equation.

The geometry of serrated chip and basic parameters in high-speed orthogonal cutting are shown in Fig. 2. The x axis is along the shear zone and y axis is perpendicular to the x axis. The momentum equation, energy equation, and compatibility condition are respectively given as Eqs. (1)–(3).

$$\rho\frac{\partial v}{\partial t}=\frac{\partial \tau}{\partial y} \tag{1}$$

$$\rho c\frac{\partial T}{\partial t}=\beta\tau\frac{\partial \gamma}{\partial t}+k\frac{\partial^2 T}{\partial y^2} \tag{2}$$

$$\dot{\gamma}=\frac{\partial v}{\partial y} \tag{3}$$

Where γ, $\dot{\gamma}$, τ, T are shear strain, shear strain rate, shear stress, and cutting temperature, respectively. v is material velocity. ρ, c, k, β, t are workpiece mass density, heat capacity, heat conductivity, the Taylor-Quinney coefficient which is approximately equal to 0.9, and time, respectively. Substituting Eq. (3) to (1), Eq. (4) can be obtained.

$$\rho\frac{\partial^2 \gamma}{\partial t^2}=\frac{\partial^2 \tau}{\partial y^2} \tag{4}$$

Upon the application of appropriate boundary conditions, the solution of Eqs. (2) and (4) leads to a steady state solution corresponding to continuous chip formation. However, other types of chip morphology, e.g. serrated chip, can be formed usually at high cutting speeds while the above solution is not a group of real number.

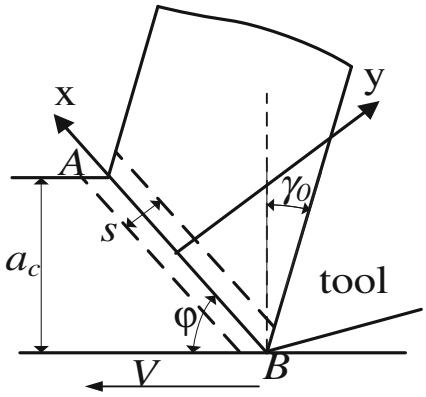

Fig. 2 Modeling of high -peed orthogonal cutting

3 Analytical characterization of ASBS

In order to study adiabatic shear instability of the homogeneous solution of governing Eqs. (2) and (4), the linear instability analysis has been used [3, 9–11]. It is supposed that:

$$\begin{cases} \gamma = \gamma^0 + \gamma' \\ \gamma' \ll \gamma^0 \end{cases}, \begin{cases} T = T^0 + T' \\ T' \ll T^0 \end{cases}, \begin{cases} \tau = \tau^0 + \tau' \\ \tau' \ll \tau^0 \end{cases} \quad (5.1\sim5.3)$$

where γ^0, T^0 and τ^0 is the solution of Eqs. (2) and (4). γ', T' and τ' are infinitesimal perturbations. The perturbations are supposed to have the forms:

$$\gamma' = \widetilde{\gamma} e^{\alpha t + iqy}, T' = \widetilde{T} e^{\alpha t + iqy}, \tau' = \widetilde{\tau} e^{\alpha t + iqy} \quad (6.1\sim6.3)$$

where $\widetilde{\gamma}$, $\widetilde{T}$ and $\widetilde{\tau}$ are the amplitude of the perturbations about shear strain, cutting temperature and shear stress, respectively, α is the corresponding growth rate, and q is the wave number. Then, the governing Eqs. (2) and (4) can be expressed as Eq. (7).

$$\left\{ \rho c \alpha \widetilde{T} = \beta \tau \alpha \widetilde{\gamma} + \beta \widetilde{\tau} \dot{\gamma} - k q^2 \widetilde{T} \rho \alpha^2 \widetilde{\gamma} = -\widetilde{\tau} q^2 \right. \quad (7)$$

It can be considered that the perturbations are produced by the chatter from the machining system of machine tool-cutting tool-workpiece. The reason of the perturbation can then be regarded as the perturbation of $\widetilde{V}$ and $\widetilde{a}_c$. The perturbation is supposed as followings.

$$\begin{cases} V = V^0 + V' \\ V' \ll V^0 \\ V' = \widetilde{V} e^{\alpha t + iqy} \end{cases}, \begin{cases} a_c = a_c^0 + a_c' \\ a_c' \ll {a_c}^0 \\ a_c' = \widetilde{a}_c e^{\alpha t + iqy} \end{cases} \quad (8.1\sim8.2)$$

where V is the cutting speed and a_c is the uncut chip thickness. The perturbation of $\widetilde{\gamma}$, $\widetilde{T}$ and $\widetilde{\tau}$ can be regarded as produced by the perturbation of cutting conditions. The relationships between $\widetilde{\gamma}$, $\widetilde{\tau}$, $\widetilde{T}$, and V, a_c can be expressed as the following:

$$\widetilde{\gamma} = \frac{\partial \gamma}{\partial V}\widetilde{V} + \frac{\partial \gamma}{\partial a_c}\widetilde{a}_c, \widetilde{T} = \frac{\partial T}{\partial V}\widetilde{V} + \frac{\partial T}{\partial a_c}\widetilde{a}_c, \widetilde{\tau} = \frac{\partial \tau}{\partial V}\widetilde{V} + \frac{\partial \tau}{\partial a_c}\widetilde{a}_c \quad (9.1\sim9.3)$$

Substituting Eqs. (9) into (7), the governing equation becomes:

$$\begin{cases} \left[(\rho c \alpha + k q^2) \frac{\partial T}{\partial V} - \beta \tau \alpha \frac{\partial \gamma}{\partial V} - \beta \dot{\gamma} \frac{\partial \tau}{\partial V} \right] \widetilde{V} + \left[(\rho c \alpha + k q^2) \frac{\partial T}{\partial a_c} - \beta \tau \alpha \frac{\partial \gamma}{\partial a_c} - \beta \dot{\gamma} \frac{\partial \tau}{\partial a_c} \right] \widetilde{a}_c \\ = 0 \left(\rho \alpha^2 \frac{\partial \gamma}{\partial V} + q^2 \frac{\partial \tau}{\partial V} \right) \widetilde{V} + \left(\rho \alpha^2 \frac{\partial \gamma}{\partial a_c} + q^2 \frac{\partial \tau}{\partial a_c} \right) \widetilde{a}_c = 0 \end{cases} \quad (10)$$

For the solution ($\widetilde{V}$, $\widetilde{a}_c$), the following characteristic equation is obtained.

$$A_3 \alpha^3 + A_2 \alpha^2 + A_1 \alpha + A_0 = 0 \quad (11)$$

The coefficients of the characteristic equation are expressed as the following:

$$A_3 = \rho^2 c \left(\frac{\partial T}{\partial V} \frac{\partial \gamma}{\partial a_c} - \frac{\partial \gamma}{\partial V} \frac{\partial T}{\partial a_c} \right) \quad (12.1)$$

$$A_2 = \rho k q^2 \left(\frac{\partial T}{\partial V} \frac{\partial \gamma}{\partial a_c} - \frac{\partial T}{\partial a_c} \frac{\partial \gamma}{\partial V} \right) + \rho \beta \dot{\gamma} \left(\frac{\partial \gamma}{\partial V} \frac{\partial \tau}{\partial a_c} - \frac{\partial \gamma}{\partial a_c} \frac{\partial \tau}{\partial V} \right) \quad (12.2)$$

$$A_1 = \rho c q^2 \left(\frac{\partial T}{\partial V} \frac{\partial \tau}{\partial a_c} - \frac{\partial T}{\partial a_c} \frac{\partial \tau}{\partial V} \right) + \beta \tau q^2 \left(\frac{\partial \gamma}{\partial a_c} \frac{\partial \tau}{\partial V} - \frac{\partial \gamma}{\partial V} \frac{\partial \tau}{\partial a_c} \right) \quad (12.3)$$

$$A_0 = k q^4 \left(\frac{\partial T}{\partial V} \frac{\partial \tau}{\partial a_c} - \frac{\partial T}{\partial a_c} \frac{\partial \tau}{\partial V} \right) \quad (12.4)$$

Table 1 Chemical composition of Ti6Al4V

Element	C	Fe	N	Al	V	H	Ti
wt.%	0.05	0.09	0.01	6.15	4.40	0.005	Base

It is a specific process that adiabatic shear instability may be produced periodically in high-speed machining. It is supposed that adiabatic shear instability occurs at the position *AB* shown in Fig. 2 at the maximum strain rate. The shear strain and shear strain rate while producing continuous chip can be expressed as the following [12]:

$$\gamma = \frac{\cos\gamma_0}{2\sin\phi\cos(\phi-\gamma_0)} \tag{14.1}$$

$$\dot{\gamma} = \frac{5.9V\sin\phi\cos\gamma_0}{a_c\cos(\phi-\gamma_0)} \tag{14.2}$$

where γ_0 is the tool rake angle and ϕ is the shear angle. The chip morphology transformation is a gradual process during machining process. The morphology of chip changes from continuous type to serrated one when adiabatic shear instability generates. The adiabatic shear instability can be ascribed to the influence of cutting speed and uncut chip thickness. Before the generation of adiabatic shear instability, the deformation can be considered as that of continuous chip. Therefore, the deformation can be expressed as Eqs. (14.1~14.2) when adiabatic shear instability is to be generated. Differentiation of shear strain γ and shear strain rate $\dot{\gamma}$ in Eqs. (14.1~14.2) with respect to cutting speed and uncut chip thickness, the Eqs. (15.1~15.4) can be obtained.

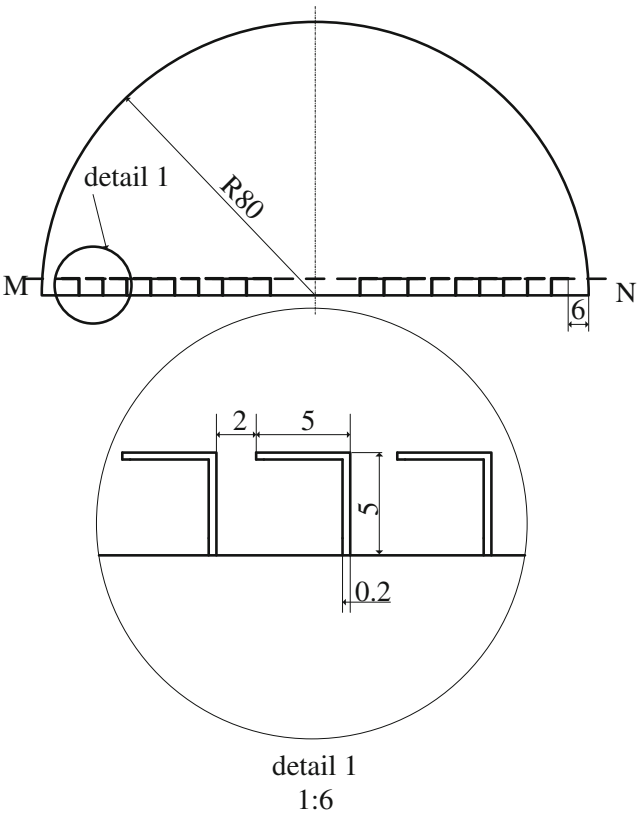

Fig. 3 Specific shape of the workpiece

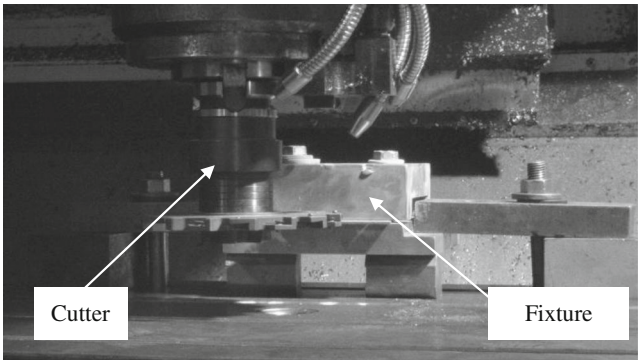

Fig. 4 Orthogonal cutting setup

$$\frac{\partial\gamma}{\partial V} = -\frac{\cos(2\phi-\gamma_0)\cos\gamma_0\ \partial\phi}{2\sin^2\phi\cos^2(\phi-\gamma_0)\partial V} \tag{15.1}$$

$$\frac{\partial\gamma}{\partial a_c} = -\frac{\cos(2\phi-\gamma_0)\cos\gamma_0\ \partial\phi}{2\sin^2\phi\cos^2(\phi-\gamma_0)\partial a_c} \tag{15.2}$$

$$\frac{\partial\dot{\gamma}}{\partial V} = \frac{5.9\sin\phi\cdot\cos\gamma_0}{a_c\cos(\phi-\gamma_0)} + \frac{5.9V\cos^2\gamma_0\ \partial\phi}{a_c\cos^2(\phi-\gamma_0)\partial V} \tag{15.3}$$

$$\frac{\partial\dot{\gamma}}{\partial a_c} = \frac{5.9V\cos^2\gamma_0\ \partial\phi}{a_c\cos^2(\phi-\gamma_0)\partial a_c} - \frac{5.9V\sin\phi\cos\gamma_0}{a_c{}^2\cos(\phi-\gamma_0)} \tag{15.4}$$

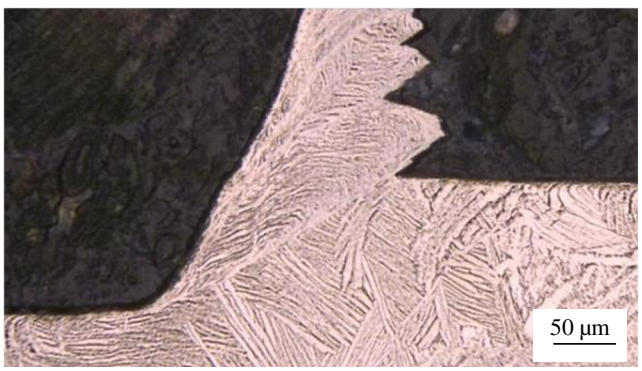

Fig. 5 Microgram of the chip root (V=50 m/min, a_c=0.1 mm)

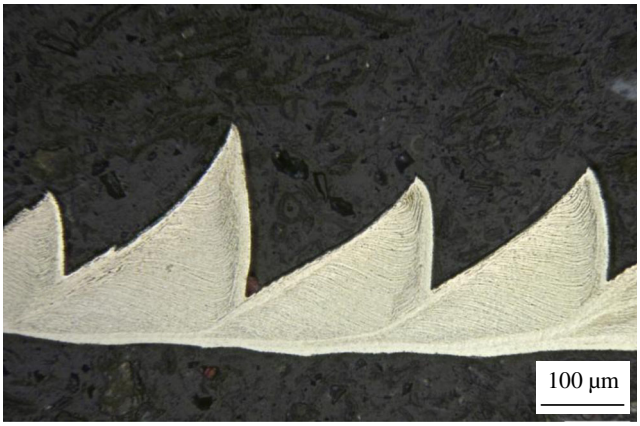

Fig. 6 Microgram of ASB (V=200 m/min, a_c=0.12 mm)

The heat produced from plastic work will not diffuse during the adiabatic shear, so the temperature in the shear zone can be expressed as Eq. (16).

$$T = \frac{\beta\tau\gamma}{\rho c} \tag{16}$$

The differentiation of the cutting temperature and the shear stress with respect to cutting speed and uncut chip thickness can then be expressed as:

$$\frac{\partial T}{\partial V} = \frac{\left(\frac{\partial\tau}{\partial\gamma}\frac{\partial\gamma}{\partial V} + \frac{\partial\tau}{\partial\dot{\gamma}}\frac{\partial\dot{\gamma}}{\partial V}\right)\gamma + \tau\frac{\partial\gamma}{\partial V}}{\rho c - \gamma\frac{\partial\tau}{\partial T}} \tag{17.1}$$

Table 2 Shear angles, ASBS, and relative error at different cutting speeds and uncut chip thicknesses

V (m/min)	a_c (mm)	φ (°)	d_e (μm)	d_t (μm)	δ_d (%)
50	0.1	35.58	200.94	212.38	5.69
100	0.1	36.68	182.66	170.42	6.70
200	0.02	34.13	56.32	63.11	12.06
200	0.04	35.47	94.32	85.23	9.64
200	0.06	36.96	115.38	102.45	11.21
200	0.08	37.43	138.83	129.87	6.45
200	0.10	38.21	178.17	166.32	6.65
200	0.12	39.34	184.39	172.36	6.52
200	0.14	39.99	194.89	200.58	2.92
200	0.16	40.63	196.53	208.36	6.02
400	0.1	40.69	147.14	137.47	6.57
600	0.1	42.60	114.68	118.98	3.75
800	0.1	44.13	110.65	108.53	1.92
1000	0.1	45.28	106.29	100.74	5.22
1300	0.1	46.24	102.16	97.63	4.43
1800	0.1	46.85	95.97	92.58	3.53

$$\frac{\partial T}{\partial a_c} = \frac{\left(\frac{\partial\tau}{\partial\gamma}\frac{\partial\gamma}{\partial a_c} + \frac{\partial\tau}{\partial\dot{\gamma}}\frac{\partial\dot{\gamma}}{\partial a_c}\right)\gamma + \tau\frac{\partial\gamma}{\partial a_c}}{\rho c - \gamma\frac{\partial\tau}{\partial a_c}} \tag{17.2}$$

$$\frac{\partial\tau}{\partial V} = \frac{\partial\tau}{\partial\gamma}\frac{\partial\gamma}{\partial V} + \frac{\partial\tau}{\partial\dot{\gamma}}\frac{\partial\dot{\gamma}}{\partial V} + \frac{\partial\tau}{\partial T}\frac{\partial T}{\partial V} \tag{17.3}$$

$$\frac{\partial\tau}{\partial a_c} = \frac{\partial\tau}{\partial\gamma}\frac{\partial\gamma}{\partial a_c} + \frac{\partial\tau}{\partial\dot{\gamma}}\frac{\partial\gamma}{\partial a_c} + \frac{\partial\tau}{\partial T}\frac{\partial T}{\partial a_c} \tag{17.4}$$

Previous studies [4, 5, 10, 13, 14] show that the wavelength is related to the wave number q when the growth rate reaches the maximum. So α_m and q should satisfy Eq. (18).

$$\frac{\mathrm{d}\alpha}{\mathrm{d}q}\Big|_{\alpha=\alpha_m} \tag{18}$$

The adiabatic shear in high-speed machining is regarded as a result of perturbation which varies with the change of time t and space (y direction). When the growth rate changes from 0 to α_m. The perturbation will reach its peak and then evolve in a periodic cycle. The wavelength when the growth rate reaches the maximum can be regarded as the ASBS. So, the ASBS is defined with Eq. (19).

$$d = \frac{2\pi}{q}|\alpha = \alpha_m \tag{19}$$

Submitting Eqs. (11)–(18) to (19), the analytical solution of ASBS is obtained. It can be found that ASBS is determined by the cutting conditions and the constitutive equation for work-piece material.

4 Experimental validation and discussion

Titanium alloy Ti6Al4V has been widely applied to aircraft engines and airframes due to its higher strength, corrosion resistance, lower density, and better thermal stability. However, Ti6Al4V is a typical difficult-to-machine material owing to its lower thermal conductivity and lower elastic modulus. Meanwhile, it is a high adiabatic shear-sensitive material at high strain rate conditions such as high-speed cutting [15, 16]. Ti6Al4V is prone to fail in the form of adiabatic shear. The

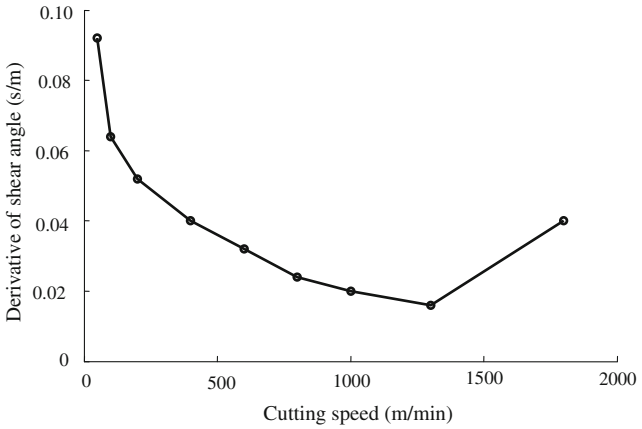

Fig. 7 Derivative of shear angle (V=50–1,800 m/min, a_c=0.10 mm)

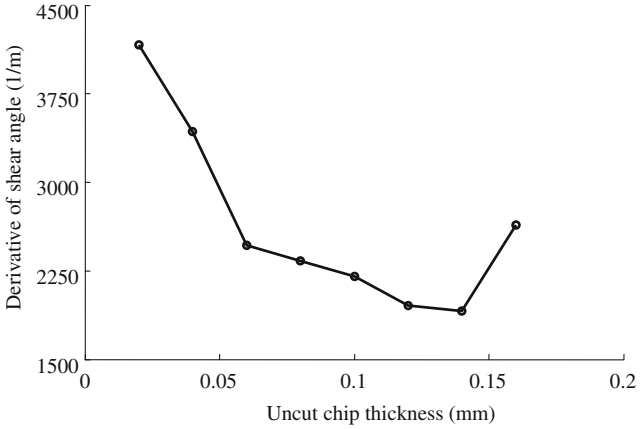

Fig. 8 Derivative of shear angle (V=200 m/min, a_c=0.02–0.16 mm)

chemical composition of Ti6Al4V is shown in Table 1. The parameters of material properties for Ti6Al4V are as listed below.

$$\rho = 4,420\text{kg/m}^3, c = 500\ \text{J/(kg K)}, k = 19\ \text{J/(m K)}$$

The basic constitutive equation adopted here is the power law constitutive equation expressed as the Eq. (20).

$$\tau = \mu_0 \gamma^n \dot{\gamma}^{\,m} T \tag{20}$$

And the parameters of the Eq. (20) for Ti6Al4V are listed below [17].

$$\mu_0 = 1.2 \times 10^{13}\text{Pa},\ \ n = 0.15, m = 0.033, \nu = -1.7.$$

The orthogonal cutting experiment was performed on a vertical machining center DAEWOO ACE-V500. A 90° SN slot milling cutter (Kennametal, 4.96164-210) was used in the cutting experiment with coated carbide (KC725M) inserts, and the type of the carbide inserts is SNHX12L5PZTNGP.

There have been several established shear angle models such as Merchant's [18], Lee and Shaffer's [19], Oxley and Welsh's [20], etc. These models have provided the relationship between the shear angle, rake angle, and friction angle. However, the friction angle is difficult to measure in the cutting process. The experimental method is used to obtain shear angles in different cutting conditions. The workpiece is the 2 mm slice, and the specific shape is shown in Fig. 3. In order to make chip roots separate from workpiece more easily, the centerline of slot milling cutter and dashed line *MN* are in the same plane. The setup of orthogonal cutting is shown in Fig. 4.

The chip roots and serrated chips of Ti6Al4V with different cutting speeds and uncut chip thicknesses have been collected after machining. Through inlay, polishing, corrosion with the corrodent 5 % of HF, 15 % of HNO_3 and 80 % of H_2O, the chip roots and serrated chips are observed with VHX-600 ESO digital microscope. The microgram of the chip root while the cutting speed of 50 m/min and the uncut chip thickness 0.1 mm is shown in Fig. 5. The ASB observed at the cutting speed of 50 m/min and the uncut chip thickness 0.12 mm is shown in Fig. 6.

The shear angles and ASBS at different cutting speeds and uncut chip thicknesses are listed in Table 2. It can be concluded from Table 2 that the shear angle increases with cutting speed and uncut chip thickness. The differentiation of shear angle with respect to cutting speed and uncut chip thickness can be approximately expressed as the following:

$$\frac{\partial \phi}{\partial V}(i) = \frac{\phi(i+1) - \phi(i)}{V_{i+1} - V_i}, \frac{\partial \phi}{\partial a_c}(j) = \frac{\phi(i+1) - \phi(i)}{a_c(i+1) - a_c(i)} \tag{21}$$

where $\frac{\partial \phi}{\partial V}(i), \frac{\partial \phi}{\partial a_c}(j)$ represent the differentiation of shear angle at some specific cutting speed and uncut chip thickness,

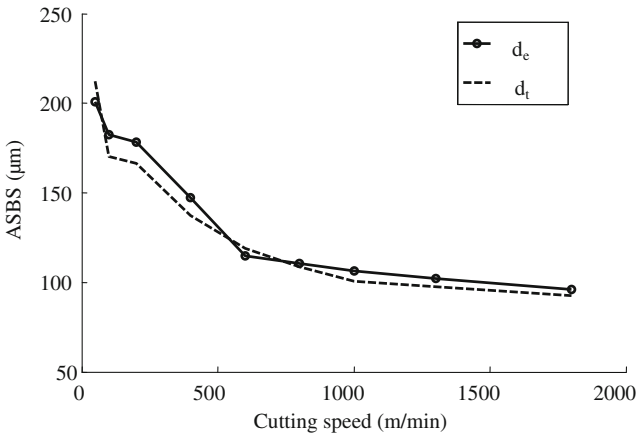

Fig. 9 ASBS of experiment and theory (V=50–1,800 m/min, a_c= 0.10 mm)

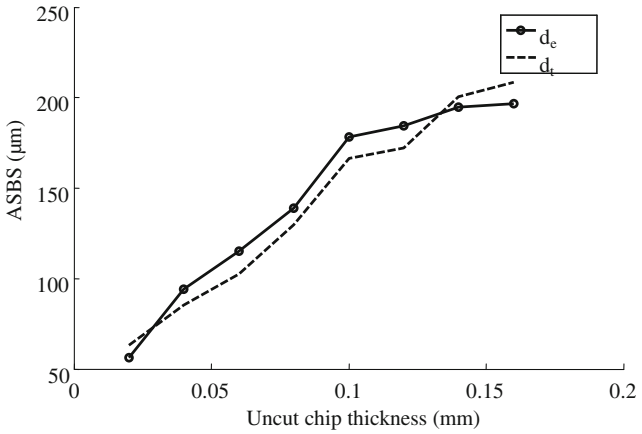

Fig. 10 ASBS of experiment and theory (V=200 m/min, a_c=0.02–0.16 mm)

respectively, $i=1\sim8$ and $j=1\sim7$. When $i=9$ and $j=8$, it is assumed as the following:

$$\frac{\partial\phi}{\partial V}(9)=\sum_{i=1}^{i=8}\frac{\partial\phi}{\partial V}(i)/8,\frac{\partial\phi}{\partial a_c}(8)=\sum_{j=1}^{j=7}\frac{\partial\phi}{\partial a_c}(j)/7 \tag{22}$$

Substituting the data of Table 2 into Eqs. (21) and (22), the curves of $\frac{\partial\phi}{\partial V}$ and $\frac{\partial\phi}{\partial a_c}$ under different conditions can be shown in Figs. 7 and 8. It is found that $\frac{\partial\phi}{\partial V}$ is in the magnitude of 10^{-2}, $\frac{\partial\phi}{\partial a_c}$ in the magnitude of 10^3 and $\frac{\partial\phi}{\partial V}\ll\frac{\partial\phi}{\partial a_c}$. The effect of uncut chip thickness is much greater than cutting speed.

Submitting Eqs. (12.1~12.4), (14.1~14.2), (15.1~15.4) and (17.1~17.4) into (11) and (19), the relationship between the growth rate α and the wave number q is established. For a given value of q, Eq. (11) has three roots and the root with largest positive real number will make the homogenous solution most unstable.

Figures 9 and 10 give the curves of ASBS measured by the experiment and computed by the proposed theory. It is found that the trend of the experimental results and the theoretical

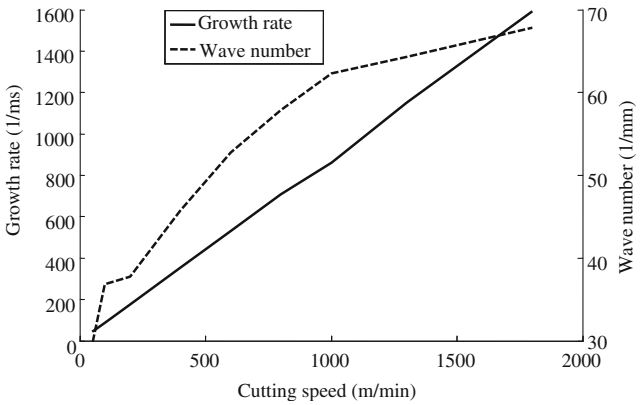

Fig. 11 Maximum of growth rate and wavelength (V=50–1,800 m/min, a_c=0.10 mm)

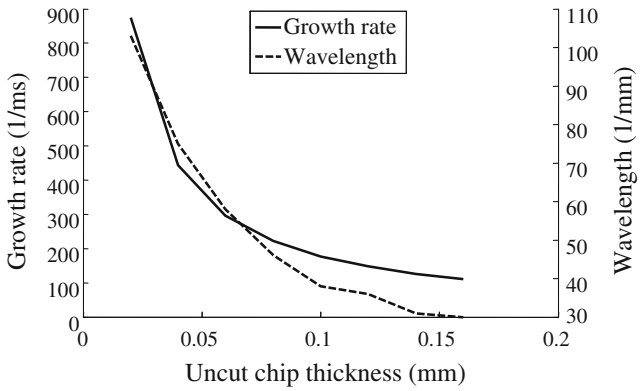

Fig. 12 Maximum of growth rate and wave length (V=200 m/min, a_c=0.02–0.16 mm)

results is consistent. ASBS decreases with cutting speed increasing and increases with uncut chip thickness. This conclusion is consistent with the literature [8], however, the prediction accuracy of ASBS under the different cutting speeds and uncut chip thicknesses may be not the same. The relative error δ_d is introduced here to represent the error of ASBS between the experimental and the theoretical value. It can be expressed as $\delta_d=|d_t-d_e|/d_e$ where d_t is the theoretical value of ASBS and d_e is the experimental value of ASBS. The values of δ_d under different cutting speeds and uncut chip thicknesses are also shown in Table 2. It can be found that the value of δ_d under different cutting speeds is a little smaller than that under different uncut chip thicknesses. When V=200 m/min and a_c=0.02 mm, the value of δ_d gets to the maximum.

The variation of the maximum growth rate α_m and the maximum wave number q_m under different cutting speeds while the uncut chip thickness is 0.1 mm is shown in Fig. 11. It is shown that both the maximum growth rate α_m and the maximum wave number q_m increases almost linearly with cutting speed and α_m increases. It is also shown that the increase of cutting speed can promote the formation of ASB. Figure 12 gives the curves of the maximum growth rate α_m and the maximum wave number q_m under different uncut chip thicknesses while the cutting speed is 200 m/min. It is indicated that α_m and q_m decreases rapidly with uncut chip thickness increasing. The maximum growth rate α_m is relative to the required time for the formation of ASB which is called the characteristic time t_c. It can be expressed that $t_c\sim1/\alpha_m$. It is found that the increase of cutting speed will accelerate the formation of ASB while the increase of uncut chip thickness will decelerate the formation of ASB.

5 Conclusion

The perturbation method has been proposed to analyze adiabatic shear instability in high-speed orthogonal cutting. A closed-form expression for ASBS has been assumed that it is related to the wavelength of perturbation having the maximum

growth rate. Results calculated from it have compared well with those obtained by the experiments. It is found that ASBS decreases with an increase of cutting speed but increases with uncut chip thickness. The maximum growth rate increases with cutting speed but decreases with an increase of uncut chip thickness. Shear angles under different cutting speeds (50–1,800 m/min) and uncut chip thicknesses (0.02–0.16 mm) during machining Ti6Al4V are obtained. It is found that the shear angle increases both with cutting speed and uncut chip thickness.

Acknowledgments The authors would like to thank National Natural Science Foundation of China (51375272 and U1201245), the Major Science and Technology Program of High-end CNC Machine Tools and Basic Manufacturing Equipment (2014ZX04012-014, 2012ZX04003-041) and National Basic Research Program of China (2009CB724401) for financial support.

References

1. Gente A, Hoffmeister HW (2001) Chip formation in machining Ti6Al4V at extremely high cutting speeds. CIRP Ann Manuf Technol 50(1):49–52
2. Batra RC, Kim CH (1992) Analysis of shear banding in twelve materials. Int J Plast 8(4):425–452
3. Wright TW, Ockendon H (1996) A scaling law for the effect of inertia on the formation of adiabatic shear bands. Int J Plast 12(7):927–934
4. Batra RC, Chen L (2001) Effect of viscoplastic relations on the instability strain, shear band initiation strain, the strain corresponding to the minimum shear band spacing, and the band width in a thermoviscoplastic material. Int J Plast 17(1):1465–1489
5. Molinari A (1997) Collective behavior and spacing of adiabatic shear bands. J Mech Phys Solids 45(9):1551–1575
6. Yang Y, Wang BF, Hu B, Hu K, Li ZG (2005) The collective behavior and spacing of adiabatic shear bands in the explosive cladding plate interface. Mater Sci Eng A 398(1–2):291–296
7. Batra RC, Wei ZG (2006) Shear band spacing in thermoviscoplastic materials. Int J Impact Eng 32(6):947–967
8. Yang Q, Liu Z, Wang B (2012) Characterization of chip formation during machining 1045 steel. Int J Adv Manuf Technol 63(9–12): 881–886
9. Bai YL (1982) Thermo-plastic instability in simple shear. J Mech Phys Solids 30(4):195–207
10. Batra RC, Chen L (1999) Shear band spacing in gradient-dependent thermoviscoplastic materials. Comput Mech 23(1):8–19
11. Daridon L, Oussouaddi O, Ahzi S (2004) Influence of the material constitutive models on the adiabatic shear band spacing: MTS, power law and Johnson-Cook models. Int J Solids Struct 41(11–12):3109–3124
12. Tay AO, Stevenson MG, de Vahl DG, Oxley PLB (1976) A numerical method for calculating temperature distributions in machining, from force and shear angle measurements. Int J Mach Tool Des Res 16(4):335–349
13. Chen L, Batra RC (1999) Effect of material parameters on shear band spacing in work-hardening gradient dependent thermoviscoplastic materials. Int J Plast 15(5):551–574
14. Batra RC, Wei ZG (2007) Instability strain and shear band spacing in simple tensile/compressive deformations of thermoviscoplastic materials. Int J Impact Eng 34(3):448–463
15. Kong F, Chen Y, Zhang D (2011) Interfacial microstructure and shear strength of Ti-6Al-4V/TiAl laminate composite sheet fabricated by hot packed rolling. Mater Des 32(6):3167–3172
16. Mahboubi Soufiani A, Enayati MH, Karimzadeh F (2010) Mechanical alloying behavior of Ti6Al4V residual scraps with addition of Al_2O_3 to produce nanostructure powder. Mater Des 31(8): 3954–3959
17. Clifton RJ, Duffy J, Hartley KA, Shawki TG (1984) On critical conditions for shear band formation at high strain rates. Scr Mater 18(5):443–448
18. Merchant ME (1945) Mechanics of the metal cutting process. I. Orthogonal cutting and a type 2 chip. J Appl Phys 16(5):267–275
19. Lee EH, Shaffer BW (1951) The theory of plasticity applied to a problem of machining. J Appl Mech-T ASME 18(4):405–413
20. Oxley PLB, Welsh MJM (1963) Calculating the shear angle in orthogonal metal cutting from fundamental stress, strain, strain-rate properties of the work material. In: Proceedings 4th International Machine Tool Design and Research Conference. Oxford, pp 73–86